

The Adamantane-Derived Bananins Are Potent Inhibitors of the Helicase Activities and Replication of SARS Coronavirus

Julian A. Tanner,^{1,6} Bo-Jian Zheng,^{2,6} Jie Zhou,² Rory M. Watt,^{1,3} Jie-Qing Jiang,¹ Kin-Ling Wong,² Yong-Ping Lin,² Lin-Yu Lu,¹ Ming-Liang He,⁴ Hsiang-Fu Kung,⁴ Andreas J. Kesel,^{5,*} and Jian-Dong Huang^{1,*}

¹Department of Biochemistry

²Department of Microbiology

³Department of Chemistry and Open Laboratory of Chemical Biology University of Hong Kong, Pokfulam Hong Kong, China

⁴Center for Emerging Infectious Diseases Faculty of Medicine

The Chinese University of Hong Kong Hong Kong, China

⁵München, Germany

Summary

Bananins are a class of antiviral compounds with a unique structural signature incorporating a trioxa-adamantane moiety covalently bound to a pyridoxal derivative. Six members of this class of compounds: bananin, iodobananin, vanillinbananin, ansabananin, eubananin, and adeninobananin were synthesized and tested as inhibitors of the SARS Coronavirus (SCV) helicase. Bananin, iodobananin, vanillinbananin, and eubananin were effective inhibitors of the ATPase activity of the SCV helicase with IC₅₀ values in the range 0.5–3 μM. A similar trend, though at slightly higher inhibitor concentrations, was observed for inhibition of the helicase activities, using a FRET-based fluorescent assay. In a cell culture system of SCV, bananin exhibited an EC₅₀ of less than 10 μM and a CC₅₀ of over 300 μM. Kinetics of inhibition are consistent with bananin inhibiting an intracellular process or processes involved in SCV replication.

Introduction

Adamantanes, formally designated tricyclo[3.3.1.1] decanes, are structurally unusual compounds where four cyclohexane rings are fused to each other in a particularly strain-free, all chair conformation. Oligo-oxa-adamantanes contain oxygens in place of methylene linkages within the structure and play a variety of roles in nature; from the infamous neurotoxin from the puffer fish *tora fugu*, tetrodotoxin (TTX) (Figure 1) [1], to plant natural product steroids such as daigremontianin [2]. Not all adamantane derivatives are extremely toxic, and many synthetic derivatives such as amantadine are used clinically (Figure 1) [3]. Amantadine is used as an antiviral agent [3], and as a muscle relaxant in the treat-

ment of Parkinson's disease [4]. Other drugs include rimantadine (against influenza A) [5], tromantadine (against herpes simplex virus), [6] and memantine (*N*-methyl-D-aspartate [NMDA] receptor antagonist) [7]. In order to add potential cytoprotective functionality [8], oligo-oxa-adamantanes have recently been conjugated to vitamin B6 (pyridoxal) to create a new class of adamantanes—the bananins (Figure 1) [9]. We have synthesized six bananin derivatives—bananin (BAN), iodobananin (IBN), adeninobananin (ADN), vanillinbananin (VBN), eubananin (EUB), and ansabananin (ABN). The synthesis of bananin was described [9], the synthesis of IBN and ADN will be reported elsewhere (A.J.K., submitted), and the final three are described in this report.

Severe acute respiratory syndrome (SARS) is caused by infection with the SARS coronavirus (SCV) [10–12]. SCV was rapidly sequenced following its identification [13, 14], leading to the recognition of a number of possible drug targets. Although treatment with ribavirin and corticosteroids has been shown to have a slight positive effect [15], side-effects [16] and lack of activity of ribavirin in cell culture [17] highlight the need for more effective treatments. Most recent anti-SCV drug development has targeted the viral main protease, also called the 3CL protease, and following an initial crystal structure [18], a structure together with inhibitors was solved [19]. Other classes of boronic-acid-based protease inhibitors have also been identified [20], and large-scale screens have identified SCV inhibitors effective against the protease [21]. We and collaborators have also recently identified inhibitors of the SCV helicase, the protease and spike-mediated viral entry by a chemical genetics approach [22]. In this paper we focus specifically on the SCV NTPase/helicase. Drugs targeting viral helicases have had marked success in animal models of herpes simplex virus [23, 24], and there has been progress in targeting the hepatitis C virus helicase [25]. We have previously cloned, purified, and performed an initial biochemical characterization of the SCV helicase [26]; our results showed that the helicase exhibited strict 5' to 3' polarity, consistent with contemporary reports from another group [27]. It has also been shown recently that the SCV helicase possesses an RNA 5'-triphosphatase activity that may be involved in capping viral RNA [28].

The SCV helicase consists of three major domains—a putative N-terminal metal binding domain (MBD), a hinge domain, and an NTPase/helicase domain. It is clear from previous work on another member of the *Nidovirales* order, equine arterivirus (EAV), that the metal binding domain is essential to viral viability [29, 30]—this is also likely to be the case for closely related SCV. In this paper, we investigate the effects of the bananin series of compounds on both the ATPase and helicase activities of the SCV helicase, and also test bananin against SCV in cell culture. We find that bananin and three of its derivatives are potent inhibitors of both the ATPase and helicase activities of the SCV helicase, and that bananin inhibits SCV replication at a concentration significantly below that at which it is toxic to the cell.

*Correspondence: andreas.kesel@t-online.de (A.J.K.); jdhuang@hkucc.hku.hk (J.-D.H.)

⁶These authors contributed equally to this work.

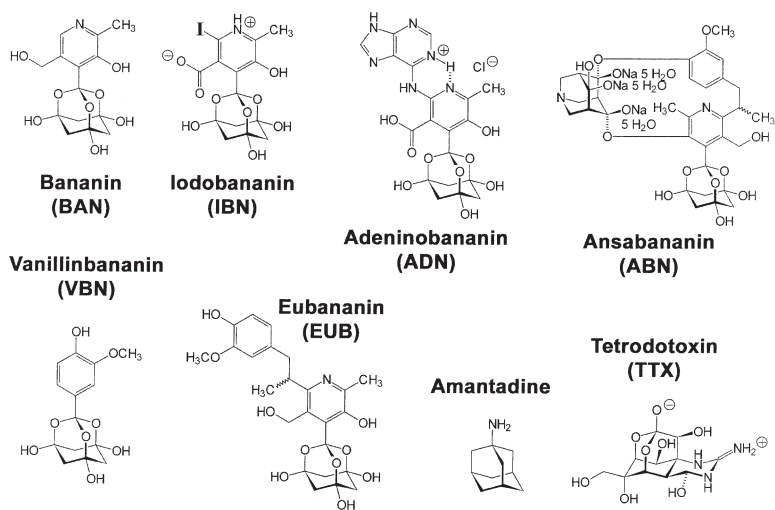


Figure 1. Chemical Structures of the Six Synthetic Bananin Derivatives (Bananin, Iodobaninin, Adeninobananin, Vanillinbananin, Eubananin, and Ansabaninin), the Anti-Influenza and Anti-Parkinson's Drug Amantadine, and the Fugu Fish Toxin Tetrodotoxin

Further cell culture studies suggest that bananin inhibits intracellular activities mechanistically involved with key viral processes, as opposed to the viral entry step. These results are consistent with this class of drugs targeting the SCV helicase within the cell.

Results

Synthesis of Bananin and Its Derivatives

The bananins were synthesized by the reaction of phloroglucinol (most likely in its triketo tautomeric form) with aromatic aldehydes, catalyzed by hydrochloric acid or sodium hydroxide in aqueous solution [9]. Generally, acidic catalysis was used due to the degradation of pyridoxal under highly basic conditions. Alkaline catalysis was used for reaction with aromatic aldehydes such as vanillin. Bananin synthesis is driven by the creation of the highly symmetric trioxa-adamantane-triol (TAT) cage system. The prototypical compound of the TAT series, the vitamin B₆-derived bananin (BAN) or 1-[3-hydroxy-5-(hydroxymethyl)-2-methyl-4-pyridinyl]-2,8,9-trioxaadamantane-3,5,7-triol, can be iodinated with subsequent oxidation to iodobananin (6'-iodobananin 5'-carboxylic acid, IBN). The iodine in IBN can be replaced by various substituents as exemplified by the synthesis of adeninobananin (6'-adeninobananin 5'-carboxylic acid hydrochloride, ADN) using an activated adenine nucleobase derivative. Interestingly, BAN is susceptible to Michael addition with the natural product eugenol, isolated from the essential oil of cloves (*Syzygium aromaticum*). This NaOH-catalyzed addition leads to eugenolbananin (eubananin, EUB), which can be transformed by cyclic hemiketal condensation into the *ansa*-compound ansabaninin (ABN), inspired by ansamycins such as rifamycin and geldanamycin [31]. In the aromatic aldehyde series, vanillin was reacted with phloroglucinol to yield vanillinbananin (VBN) or 1-(4-hydroxy-3-methoxyphenyl)-2,8,9-trioxaadamantane-3,5,7-triol. It is expected that numerous naturally occurring aldehydes can be introduced to form the corresponding TATs with phloroglucinol in 3.33 M aqueous NaOH. The bananin group of compounds represents, to

our knowledge, an array of completely new adamantane derivatives, which may be easily diversified by reacting various aromatic aldehydes with phloroglucinol.

Inhibition of SCV Enzymatic Activity

We have previously developed a colorimetric assay to measure the NTPase activity of the SCV helicase in 96-well plates, in a high throughput format [26, 32, 33]. In this discontinuous colorimetric assay using malachite green and ammonium molybdate, released phosphate is quantified after a 5 min reaction period, observed at a wavelength of 630 nm. Oligo-dT₂₄ was included in the assay at a saturating concentration of 200 nM, to mimic the nucleic acid-stimulated NTPase activity of the SCV helicase. Potential inhibitors of the ATPase reaction would be expected to reduce the amount of phosphate released during the reaction, reflected in a decrease in the measured absorbance at 630 nm.

We first checked whether the bananin compounds were able to inhibit the dT₂₄-stimulated ATPase activity of the SCV helicase. Controls were carried out to ensure that the bananin compounds themselves did not affect the phosphate measurement assay. Reactions were carried out in the presence of various concentrations of the six bananin derivatives and the results were plotted and fitted to a simple model (Figure 2A). We also checked that under our reaction conditions, we were making measurements within the linear region (Figure S1).

Our results showed that the parent compound bananin inhibited the ATPase activity of the SCV helicase with an ^{ATPase}IC₅₀ value of 2.3 μM (IC₅₀ values shown in Figure 4C). Iodobananin and vanillinbananin exhibited the strongest inhibition, with ^{ATPase}IC₅₀ values of 0.54 and 0.68 μM, respectively. Inhibition by vanillinbananin indicates that the presence of a six-membered nitrogen heterocycle is not absolutely essential for inhibitory activity. Eubananin showed similar inhibitory activity to bananin itself with an ^{ATPase}IC₅₀ of 2.8 μM. Interestingly, ansabaninin was a weak inhibitor, with an ^{ATPase}IC₅₀ of 51 μM, while adeninobananin did not show any inhibitory activity at all. These results suggest that

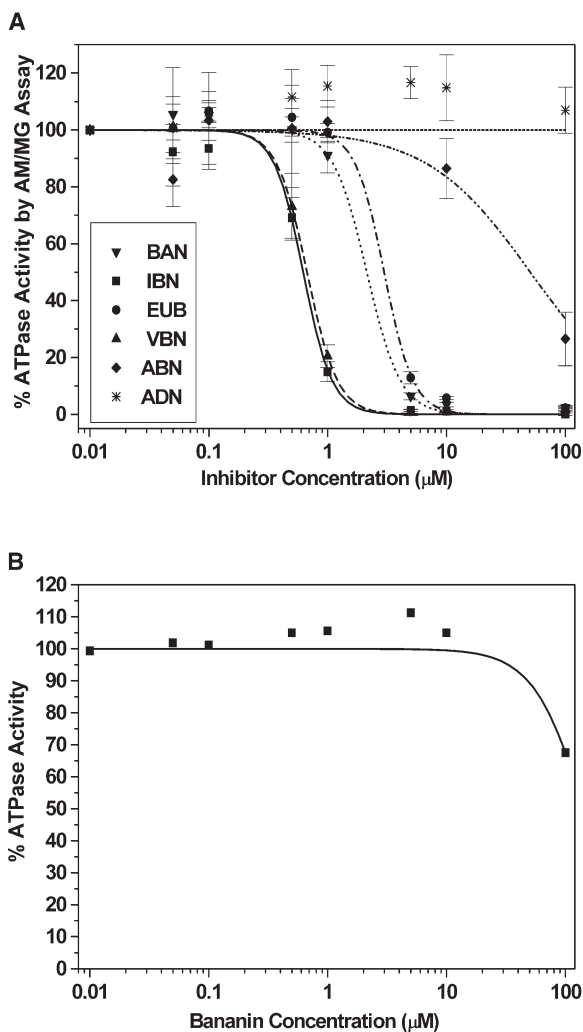


Figure 2. Inhibition of SCV Helicase ATPase Activity by the Six Different Bananin Derivatives and Inhibition of the Nonstimulated ATPase Activity by Bananin

(A) Inhibition of dT₂₄-stimulated ATPase activity. A colorimetric assay was used to measure phosphate release due to ATP to ADP hydrolysis after a 5 min period. Points shown are the average of triplicate experiments and the error bars represent the standard distribution. Data were fitted with the logistic equation to calculate each IC₅₀. (B) Inhibition of nonstimulated ATPase activity. The same assay was used to measure inhibition of the reaction in the absence of dT₂₄ by bananin.

bulky side groups on the six-membered ring of this class of compounds reduce their inhibitory activity against the SCV helicase.

We also checked whether bananin would inhibit the unstimulated basal ATPase activity in the absence of dT₂₄ of the SCV helicase (Figure 2B). It is clear that bananin is not an effective inhibitor of the unstimulated ATPase activity, although slight inhibition was observed at 100 μM.

We then tested the mechanism of inhibition of the ATPase activity by bananin, and checked competition with respect to both ATP (Figures 3A and 3B) and with respect to dT₂₄ (Figures 3C and 3D). Figures 3B and 3D

are the double reciprocal Lineweaver Burke plots for the data in Figures 3A and 3C. In both cases, as the V_{max} was significantly decreased in the presence of the inhibitor, but the K_M changed little, this indicated that bananin was acting as a noncompetitive inhibitor of the ATPase activity of the SCV helicase with respect to both ATP and nucleic acid. This suggests that bananin inhibits by binding at a site distinct from the ATP and nucleic acid binding sites.

Building on this foundation, we next tested the anti-helicase activities of these compounds. We used a newly developed fluorimetric assay based on the very strong fluorescence resonance energy transfer (FRET) from the fluorophore Cy3 to the quencher Black Hole Quencher 2 (BHQ2). A similar approach has been outlined very recently in assaying the hepatitis C virus (HCV) helicase, a 3' to 5' helicase [34]. However, as we have recently shown that the SCV helicase holds strict 5' to 3' directionality [26], we designed a system with a 5'-oligo(dT) overhang. The principle behind this assay is outlined in Figure 4A. There is a Cy3 fluorophore at the 3' end of one of the oligomers of the duplex, in close proximity to a BHQ2 quencher at the 5' end of the other oligomer. When the two oligomers are in very close proximity (i.e., when the two oligomers are annealed), then the Cy3 fluorescence is strongly quenched by the FRET effect. After the duplex has been unwound by the SCV helicase, then the Cy3 fluorescence is no longer quenched, and a dramatic increase in the fluorescence may be observed. To ensure that the primers do not reanneal, a second capture primer is included in the reaction. This is identical to the BHQ2 primer but does not contain the BHQ2 quenching group, therefore the annealing process has little effect on the fluorescence of Cy3. We optimized reaction conditions to ensure that all measurements were carried out in the linear region (Figure S2). As a one minute time-point was in the linear region, we then probed the effect of the presence of various concentrations of the bananin inhibitors and compared them to control reactions where no inhibitor was added (Figure 4B). Additional controls were carried out to verify that the bananin compounds did not fluoresce themselves at the wavelength at which we were reading. Data from these experiments were fitted to the logistic equation to obtain the ^{helicase}IC₅₀ values (Figure 4C). Although the overall ^{helicase}IC₅₀ values appeared slightly weaker (i.e., larger) than the ^{ATPase}IC₅₀ values, it was observed that the inhibitors followed the same general trends as those observed for the ATPase data. Bananin, iodobananin, vanillinbananin, and eubanin were effective inhibitors of helicase activity, while ansabanin and adenobananin barely inhibit the reaction.

We also performed a final control to check whether bananin acted as a general helicase inhibitor or not. We cloned and purified the *E. coli* DnaB helicase, which is a well characterized helicase with 5' to 3' polarity of unwinding [35]. The purity of DnaB may be observed by SDS-PAGE in Figure S3A. We found that 250 μM bananin did not inhibit DnaB in our FRET-based assay (Figure S3B). These results suggest that bananin does not act as a general helicase inhibitor.

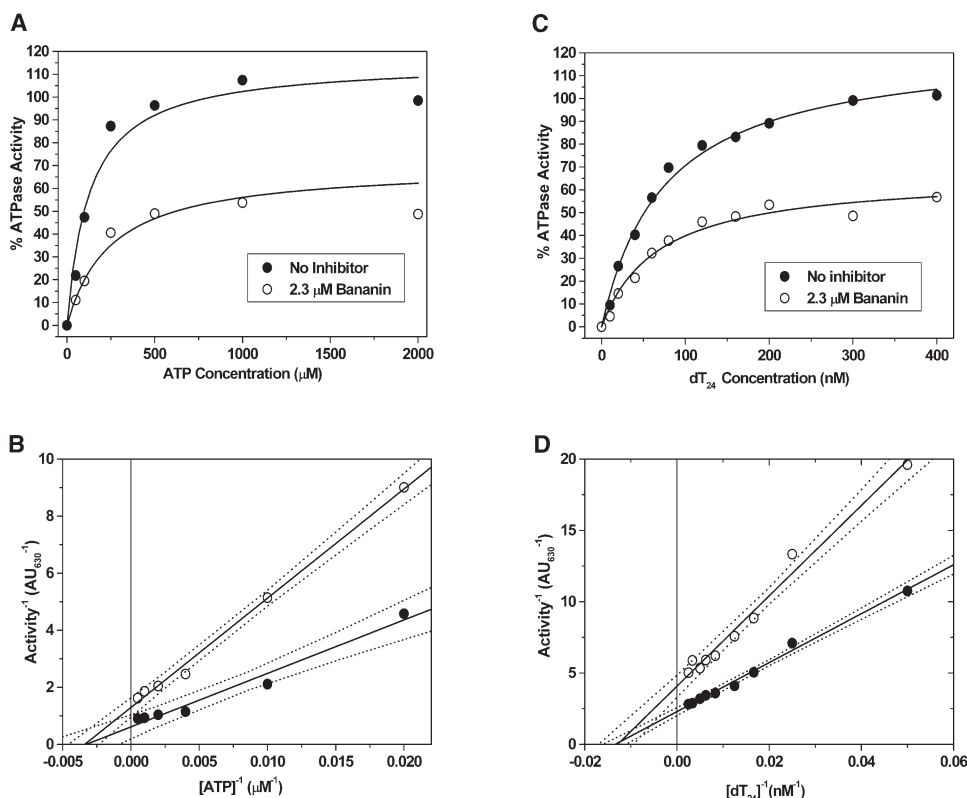


Figure 3. Bananin Is a Noncompetitive Inhibitor with Respect to Both ATP and to Nucleic Acid

Points are an average of triplicate experiments. (A) ATPase activity was measured under varying ATP concentrations in the presence and absence of 2.3 μM bananin. (B) Lineweaver Burke plot of inhibition data from (A). Solid circles represent absence of inhibitor while open circles represent presence of 2.3 μM bananin. Dotted lines represent 95% confidence of fit of straight lines. (C) ATPase activity was measured under varying dT_{24} concentrations in the presence and absence of 2.3 μM bananin. (D) Lineweaver Burke plot of inhibition data from (C). Solid circles again represent absence of inhibitor while open circles represent presence of 2.3 μM bananin. Dotted lines represent 95% confidence of fit of straight lines.

Inhibition of SARS Coronavirus Replication

The potency of these inhibitors against the SCV helicase enzymatic activities prompted us to investigate their ability to inhibit SCV replication in a cell culture system. We chose to test bananin itself, it being the most representative of the class and the parent compound. SCV has previously been established in fetal rhesus kidney-4 cells (FRhK-4) in our laboratories [36]. SCV infection typically presents clear cytopathic effects (CPEs): the cells appear inflamed with “ridged” cell membranes when infected with the virus. Visual inspection of cell cultures infected with SCV in the presence of 50 μM bananin, revealed that CPEs were distinctly reduced relative to those of a control infection (results not shown). However, levels of CPEs were difficult to quantify accurately, and so an alternative procedure was pursued.

To quantify the antiviral activity of bananin, we measured the viral titre under different inhibitor concentrations (Figure 5). The infectivity of the virus in the cultures in the presence and absence of bananin was measured by a standard TCID_{50} protocol using serial dilution of the cell culture supernatant [36], and compared to virus controls where no drug was added. Briefly, cell culture supernatant at various time points

after infection was serially diluted and fresh FRhK-4 cells were infected with the serial dilutions. Cytopathic effects were observed three days after infection with the serial dilutions, thereby allowing measurement of the viral titre. In this study, drugs were added either one hour before or one hour after the infection with a 0.03 multiplicity of infection (MOI) of the virus. In FRhK cells, the generation time of the SCV replication has been shown to be 17–19 hr (our unpublished data). Therefore, the readings at 24 hr are effectively after a single generation. It can be seen from this data that at a concentration of 10 μM bananin, the viral titre was reduced by almost 50% after 24 hr (Figure 5), and the drug was most effective when added one hour after infection compared to one hour before. When drug was added before, it was not removed on addition of the virus and was present for the rest of the experiment. After 48 hr, the difference between addition of drug before and after infection became more pronounced, and the viral titre had dropped below 35% of the control in the absence of inhibitor (Figure 5). At a concentration of 50 μM , these effects were more pronounced; when the drug was added one hour after infection, the viral titre was below 10% of an untreated control infection after 24 hr. At 100 μM bananin, the viral titre was almost zero

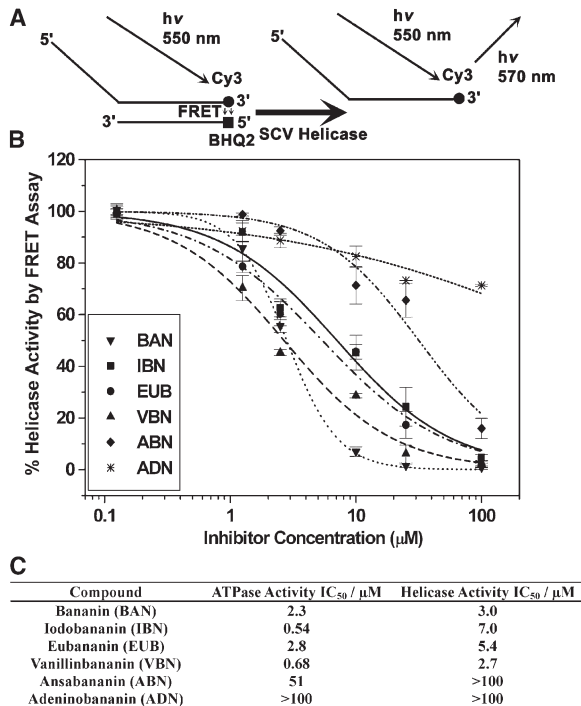


Figure 4. Principle of the FRET-Based Helicase Assay, Inhibition of SCV Helicase Activity by the Six Different Bananin Derivatives, and Summary of Enzymatic Inhibition Data

(A) Schematic showing the principles behind the FRET-based fluorimetric assay of helicase activity.

(B) Inhibition of the helicase activity of the SCV helicase in the presence of various concentrations of the six bananin derivatives. Points shown are the average of triplicate experiments. Data were fitted with the logistic equation to calculate each IC_{50} . Error bars represent the standard deviation of triplicate measurements.

(C) Table showing the IC_{50} values for inhibition of both ATPase and helicase activities of the SCV helicase.

after 24 hr and 48 hr. These results suggest first that bananin is an effective inhibitor with an EC_{50} of below $10 \mu\text{M}$ (when measured 48 hr post-infection) and when drug was added one hour after virus infection). Second, due to the increased efficacy of the drug when added post infection, these results suggest that bananin does not inhibit the entry step, but inhibits a later step of the infection cycle after the virus has penetrated the cell.

As a further assay, we used quantitative real time PCR to measure the relative quantities of viral RNA (specified by primers targeted to the SCV S-gene) compared to cellular RNA (specified by primers targeted to the gene β -actin). β -actin is expressed stably at basal level in FRhK-4 cells as determined by Q-RT-PCR and is therefore a good control for possible bias in the experiment. Again, the drug was added to various concentrations either one hour before, or one hour after infection, and compared to a control where no drug was added (Figure 6). Bananin was maintained at the same concentration throughout the experiment. The kinetics of infection were examined by making Q-RT-PCR measurements 1 hr, 6 hr, 12 hr, 24 hr, and 48 hr post-infection. Up to 6 hr post infection, there was little difference in SCV S-gene levels between the control and

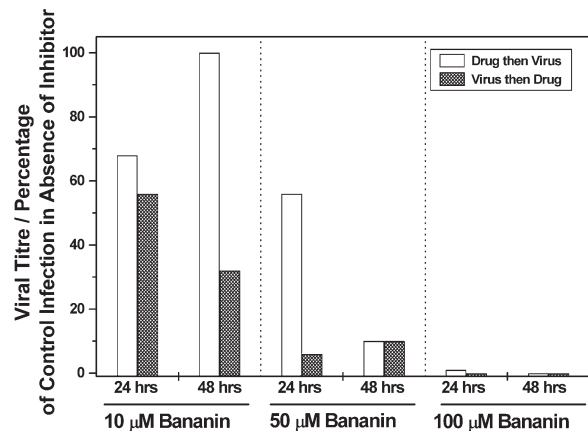


Figure 5. The Antiviral Activities of Bananin Measured by 50% Tissue Culture Infective Dose (TCID_{50})

Bananin was added to cultures at the concentration indicated either one hour before (white bars) or one hour after (hatched bars) infection with the virus. The TCID_{50} was measured either 24 hr or 48 hr after infection by a standard serial dilution protocol and compared to a control where the culture had been infected in the absence of inhibitor.

in the cultures containing bananin, even at a concentration of $100 \mu\text{M}$ (Figure 6). However, after 12 hr, it was clearly observed that the drug was having an inhibitory effect, even at a concentration of $10 \mu\text{M}$, and this effect increased with time up to 48 hr. This data also indicated that adding the drug after viral infection was considerably more effective than when it was added before (Figure 5).

We measured the toxicity of bananin using a standard MTT assay. Fitting the logistic equation to the data

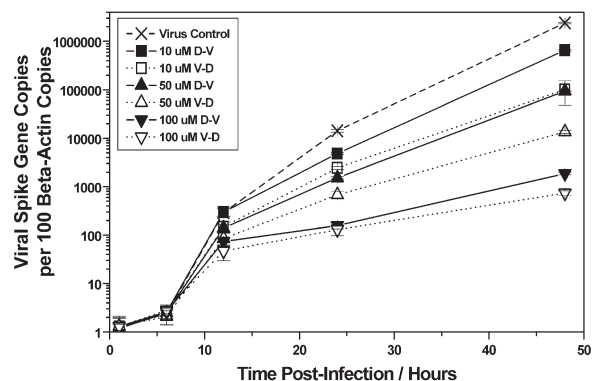


Figure 6. Kinetics of the Antiviral Activity of Bananin Measured by Quantitative Real Time PCR

Bananin was added to cultures at the concentration indicated (square: $10 \mu\text{M}$, up triangle: $50 \mu\text{M}$, down triangle: $100 \mu\text{M}$) either 1 hr before (D-V represents drug then virus, filled symbols) or 1 hr after (V-D represents virus then drug, open symbols) infection with the virus. Cellular and viral RNA levels were measured by quantitative real time PCR over a 48 hr period, using primers complementary to the β -actin and SCV Spike protein genes, respectively, and are displayed using a logarithmic scale. A control in the absence of inhibitor was also carried out (crosses). Error bars represent the standard deviation of triplicate measurements.

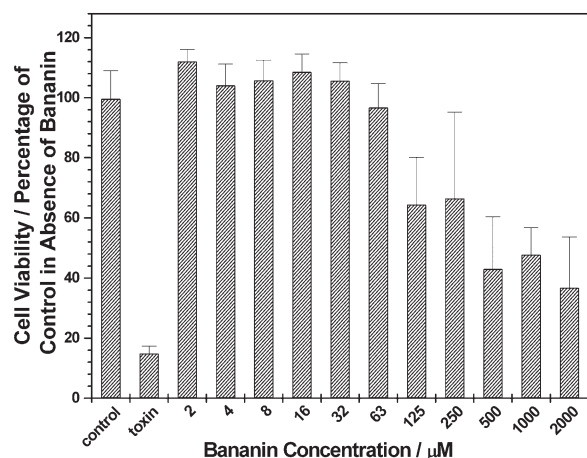


Figure 7. Toxicity of Bananin to FRhK-4 Cells As Measured Using the MTT Assay

Cell viability was measured after 48 hr in the presence of the indicated concentrations of bananin by the MTT assay. Toxin represents amanitin at 30 $\mu\text{g/ml}$. Error bars represent the standard deviation of five measurements.

indicated that 48 hr post infection, bananin exhibited a cytotoxic concentration causing 50% cell mortality (CC_{50}) of 390 μM (Figure 7). As the EC_{50} for bananin added post infection at 48 hr was less than 10 μM (Figure 5B), this result implies a specificity index ($\text{CC}_{50}/\text{EC}_{50}$) of over 39.

Discussion

Here we describe the synthesis and inhibitory effects against enzymatic activities of the SARS coronavirus helicase for several structurally unusual trioxa-adamantane derivatives, trivially referred to as bananins. We also show that bananin exhibits significant anti-SCV activity in cell culture, through the inhibition of a process occurring after viral entry into the cell. We have developed an extremely convenient and quick method for testing both ATPase activities colorimetrically, and helicase activities fluorimetrically through a type of FRET assay. This combination of assays may be adapted easily for high-throughput screening of compound libraries against both NTPase and DNA-unwinding enzymatic activities, and avoids the use of radioactive ^{32}P , which is commonly used in many traditional helicase assays.

ATPase assays revealed that iodobananin and vanillinbananin were the most effective SCV helicase inhibitors, with $^{\text{ATPase}}\text{IC}_{50}$ values of 0.54 μM and 0.68 μM , respectively. Bananin ($^{\text{ATPase}}\text{IC}_{50} = 2.3 \mu\text{M}$) and eubananin ($^{\text{ATPase}}\text{IC}_{50} = 2.8 \mu\text{M}$) were also reasonable inhibitors, but ansabanin and adenobananin, which contain bulky appendages on the pyridoxal system, showed little if any inhibition. Bananin acted as a noncompetitive inhibitor with respect to both ATP and nucleic acid, suggesting this class of inhibitors binds at a site distinct from the ATP and nucleic acid binding sites. Far weaker inhibition of the unstimulated ATPase activity was observed, showing that bananin does not act as a

nonspecific aggregator. The ATPase inhibition results were consistent with those from the helicase assays: bananin, vanillinbananin, eubananin, and iodobananin were the best inhibitors of DNA-unwinding, while ansabanin and adenobananin were poor inhibitors. Generally, the helicase inhibition activities measured for each compound, as determined by IC_{50} values, were less than the corresponding ATPase inhibition activities, but the trends remained consistent. This appears to be a characteristic common to many helicase inhibitors [24, 25].

Bananin, which acted as an effective inhibitor in both enzymatic assays and is the prototypical member of this class of compounds, was tested in a cell culture system of the virus. Bananin exhibited antiviral effects at concentrations significantly below those causing cell toxicity ($\text{EC}_{50} < 10 \mu\text{M}$, $\text{CC}_{50} = 390 \mu\text{M}$). Experiments measuring the viral titer in two different situations, one where the drug was added one hour before viral infection, and one where the drug was added one hour after viral infection, suggested that bananin did not inhibit viral entry but inhibited some key intracellular processes involved in viral replication or pathogenesis. These experiments were further confirmed by kinetic experiments measuring the relative quantity of viral RNA compared to cellular RNA over 48 hr. The drug had little effect on RNA levels during the early stages of the life cycle (approximately 0–6 hr post infection), indicating that the amount of the virus which has entered the cells was similar in the presence or absence of the drug. But the viral RNA levels were very different during the later stages (from approximately 12–48 hr), suggesting that viral transcription/replication was inhibited by bananin. It is interesting to note the marked reduction in efficacy when bananin is added prior to viral infection, despite its continued presence post infection. First, this would suggest that the compound does not inhibit a viral entry process. Second, it suggests that bananin may be affecting other cellular pathways that in the absence of viral infection may resist the protective effects of the drug. The SCV helicase is one possible target within the cell, although at this stage we cannot exclude the possibility that bananin may be inhibiting via other pathway(s).

Significance

Adamantane derivatives have been used clinically for many years as antiviral treatments and as muscle relaxants. Here, we have demonstrated that a class of pyridoxal-conjugated trioxaadamantanes, the bananins, inhibit both the ATPase and helicase activities of the SARS coronavirus helicase. Testing a number of bananin derivatives, we have shown that it is important to reduce steric hindrance around the pyridoxal ring for effective inhibition of the SCV helicase. Furthermore, bananin was shown to be an effective antiviral drug in a cell culture of the virus. The mode of viral inhibition supports the hypothesis that the SCV helicase is a target of these compounds. Given the paucity of drugs shown to be effective in treating this recently emerged disease, the bananins repre-

sent a class of compounds with significant therapeutic potential against SARS.

Experimental Procedures

Synthesis of Eugenolbananin (Eubananin, EUB) from Bananin and Eugenol

A mass of 4.41 g bananin [9] ($M = 327.29$ g/mol) (13.4743 mmol) and 3.00 ml eugenol (3.20 g) ($M = 164.20$ g/mol) ($\rho_4^{20} = 1.0664$ g/ml) (19.4836 mmol) were suspended in 30 ml of water. Then, 6.00 g of sodium hydroxide (NaOH) pearls (0.15 mol) were added in small portions, then heated until all material had dissolved. Then 15.0 ml of 10 M hydrochloric acid (0.15 mol HCl) was added in small portions. The mixture was kept at 4°C for 12 hr and a precipitate recovered by filtration and desiccation. Yield: 5.33 g (81%) reddish-brown powder 1-[6-[(2RS)-1-(4-hydroxy-3-methoxyphenyl)-2-propyl]-3-hydroxy-5-(hydroxymethyl)-2-methyl-4-pyridinyl]-2,8,9-trioxadadamantane-3,5,7-triol (eubananin, EUB) $C_{24}H_{29}NO_{10}$ ($M = 491.49$ g/mol). The structure was established by a COSY combination of 1H -NMR and ^{13}C -NMR spectroscopy.

"One Pot Synthesis" of AZTRION

Masses of 18.44 g vanillin ($M = 152.14$ g/mol) (121.20 mmol) and 15.29 g phloroglucinol ($M = 126.11$ g/mol) (121.24 mmol) were suspended in 73 ml of water. Then, 29.27 g of solid sodium hydroxide pearls (NaOH) ($M = 40.00$ g/mol) was added in small portions. Immediately after the solidification, 100 ml of water was added and the suspension was shaken vigorously for 5 min until the development of heat ceased and the mixture turned crystalline. Then a mass of 22.28 g 1,3,5,7-tetraazatricyclo[3.3.1.1^{3,7}]decane (methenamine, urotropin, hexamethylenetetramine) ($M = 140.19$ g/mol) (158.93 mmol), 173 ml of water, and 39.93 g NaOH was added and the mixture was refluxed for 20 min before cooling at -18°C for 6 hr. Yield: 22.16 g (66%) fine reddish-orange needles disodium 6,10-dihydroxy-6,10-dioxido-1-azatricyclo[3.3.1.1^{3,7}]decane-4-one monohydrate [1-azaadamantane-4,6,10-trione bis(sodium hydroxide) adduct monohydrate, AZTRION] $C_9H_7NO_5Na_2 \cdot H_2O$ ($M = 277.18$ g/mol). The structure was established by a COSY combination of 1H -NMR and ^{13}C -NMR spectroscopy, supplemented by IR spectroscopy.

Synthesis of the Ansa Compound Ansabanin (ABN) from Eubananin and AZTRION

A mass of 1.17 g eubananin ($M = 491.49$ g/mol) (2.3805 mmol) was dissolved in 40.0 ml of 0.5 M sodium hydroxide aqueous solution. A mass of 1.21 g AZTRION ($M = 277.18$ g/mol) (4.3654 mmol) was added. The black solution was treated dropwise with 3.50 ml of 10 M hydrochloric acid. Afterward, 2.00 g of NaOH pearls ($M = 40.00$ g/mol) (50 mmol NaOH) was added. The black solution was kept at 4°C in an open crystallization dish for two days. After that time, the dark crystalline mass was harvested and pressed between filter papers. The material was recrystallized from 30.0 ml 2.0 M NaOH aqueous solution. The black solution was kept at 4°C in an open crystallization dish for two days. Yield: 2.43 g (99%) tan crystals disodium (\pm)-rel-[6R,10S-(R_p,R_d)]-6-exo,10-exo-dioxido-6-endo,10-endo-[1-[5-(hydroxymethyl)-6-[(2RS)-1-(3-methoxyphenyl)-2-propyl]-2-methyl-4-pyridinyl]-2,8,9-trioxadadamantane-3,5,7-triol-3',4''-diylidioxy]-1-azaadamantane-4-one sodium hydroxide adduct pentadecahydrate (ansabanin, ABN) $C_{33}H_{36}N_2O_{13}Na_2 \cdot NaOH \cdot 15 H_2O$ ($M = 1024.86$ g/mol). The structure was established by a COSY combination of 1H -NMR and ^{13}C -NMR spectroscopy.

Preparation of Vanillinbananin (VBN) from Vanillin and Phloroglucinol

Masses of 25.20 g vanillin ($M = 152.14$ g/mol) (165.64 mmol) and 20.88 g phloroglucinol ($M = 126.11$ g/mol) (165.57 mmol) were dissolved in 300 ml of water. Then 40.00 g of solid sodium hydroxide (NaOH) ($M = 40.00$ g/mol) (1 mol NaOH) was added in small portions, and, afterward, the mixture was titrated with 100 ml of 10 M hydrochloric acid (1 mol HCl). It was subsequently cooled at 4°C for 6 hr. Yield: 45.17 g (87%) yellow powder 1-(4-hydroxy-3-methoxyphenyl)-2,8,9-trioxadadamantane-3,5,7-triol or 1-(4-hydroxy-3-methoxyphenyl)-2,8,9-trioxatricyclo[3.3.1.1^{3,7}]decane-3,5,7-triol

$C_{14}H_{16}O_8$ ($M = 312.27$ g/mol). The structure was established by a COSY combination of 1H -NMR and ^{13}C -NMR spectroscopy, supplemented by UV/VIS spectrophotometry.

Cloning and Purification of the SCV Helicase

The SCV helicase domain (nsp13-pp1ab, accession number NP_828870, originally denoted as nsp10) was cloned and purified as previously described [26].

Cloning and Purification of *E. coli* DnaB

The DnaB helicase was amplified by PCR from *E. coli* genomic DNA using 5'-GGCGAATTCATGGCAGGAAATAAACCTTCAAC-3' and 5'-TAATATCTCGAGTCATTCGTGCTGCTACTGCGGCC-3'. The PCR product was gel purified then EcoRI/XhoI ligated into pET28a to form plasmid DnaB-pET28a. The plasmid was maintained in strain DH10B and transformed into strain BL21-DE3 for expression. A 5 ml LB culture containing 50 μ g/ml kanamycin was grown overnight, then 1 ml of the overnight culture was added to 500 ml LB containing 50 μ g/ml kanamycin. The culture was induced with 0.5 mM IPTG at AU = 0.4, then grown further for three hours at 37°C. The cells were collected by centrifugation and sonication was used to split soluble and insoluble fractions. DnaB was observed by SDS-PAGE to be mainly present in the insoluble fraction, and further purification was from the insoluble fraction. The insoluble fraction was washed three times with 30 ml 50 mM TRIS-HCl (pH 7.4). The pellet was then dissolved in 15 ml 6 M GuCl / 50 mM TRIS-HCl (pH 7.4)/20 mM imidazole, and any insoluble material removed by centrifugation. The protein was refolded by injecting 15 ml solution through a fine-bore needle into 135 ml of rapidly vortexing 50 mM TRIS-HCl (pH 6.8) / 5 mM MgCl₂ / 20% glycerol / 1% triton / 10 mM β -mercaptoethanol on ice. Very little precipitate was seen in this procedure; any precipitate was removed by centrifugation. The protein was then passed onto a 5 ml Ni-NTA column, washed with 50 ml of 50 mM TRIS-HCl (pH 8.5) / 40 mM imidazole, before being eluted with 50 mM TRIS-HCl (pH 8.5) / 200 mM imidazole. β -mercaptoethanol was then added to 10 mM, glycerol added to 20%, and the protein was stored at -20°C.

ATPase assays were performed using a phosphomolybdate-malachite green assay described previously [26]. Reaction conditions were 50 mM TRIS-HCl (pH 6.8), 5 mM MgCl₂, 200 nM dT₂₄ (for stimulated reactions), 0.1 mg/ml BSA, 3.2 ng SCV helicase (for stimulated) or 32 ng SCV helicase (for nonstimulated) in a 50 μ l reaction volume for 5 min in a 96-well plate. Reaction was stopped by addition of EDTA to 50 mM, then AM/MG reagent and trisodium citrate were added as described to measure phosphate released in the reaction [26]. Titration of ATPase activity with inhibitors in the presence of fixed concentrations of polynucleotide and ATP was described by a modified logistic equation [37].

$$A([L]) = 1 - \frac{\Delta A_{\infty}[L]}{EC_{50} + [L]}$$

FRET-Based Helicase Assays

We used a protocol modified from that described [34], using oligomers suitable for a 5' to 3' helicase. Two oligomers were synthesized and purified by HPLC: DT20Cy3 (5'-TTTTTTTTTTTTTTTTTTTTCGAGCACCGCTGCGGCTGCACC(Cy3)-3'), and ReleaseBHQ (5'-(BHQ2)GGTGCAGCCGCGAGCGGTGCTCG-3') (Proligo). The two oligomers were annealed by mixing a 1:1.2 ratio of DT20Cy3:ReleaseBHQ at a concentration of 8.2 μ M (of DT20Cy3) in 10 mM TRIS-HCl (pH 8.5), heating to 90°C, then cooling slowly to 40°C over one hour. The reaction was carried out in a 1 ml volume of 5 mM DT20Cy3:ReleaseBHQ, 10 nM Release oligomer (5'-GGTGCAGCGCACCGGTGCTCG-3'), 0.5 mM ATP, 0.1 mg/ml BSA, 2 nM SCV helicase, 5 mM MgCl₂, and 50 mM TRIS-HCl (pH 6.8) at 25°C for 1 min. The change in fluorescence (excitation 550 nm, emission 570 nm) after 1 min was used to monitor the extent of unwinding of the duplex. The DnaB FRET assay was carried out with 10 μ g DnaB under the same conditions.

Cell Culture and Determination of Cytopathic Effects

Fetal rhesus kidney (FRhK-4) cells were plated on a 96-well plate (2000 cells per well) under minimum essential medium containing

5% (v/v) fetal bovine serum, 1% (w/v) sodium pyruvate, 100 U/ml penicillin, 0.1 mg/ml streptomycin and were cultured at 37°C in 5% CO₂. To test anti-SCV activities, FRhK-4 cultures were treated with a range of different drug concentrations one hour before or after infection with 0.03 MOI of SCV (strain GZ50). Either 24, 36, or 48 hr post infection, cytopathic effects (CPE) were observed by phase-contrast microscopy. The uninfected cells appeared smooth while infected cells showed prominent ridge-like structures along the membranes. Viral reproduction in the infected cells was quantified by virus titration, as described below.

Inhibition of SCV Reproduction

FRhK-4 cell cultures were infected with SCV one hour before or after being treated with various concentrations of drug. Following incubation for 24 and 48 hr, viable SCV production was measured by back titration of the culture media supernatant using a TCID₅₀ (50% tissue culture infectious dose) protocol [36]. Briefly, the supernatant was serially 10-fold diluted with fresh cell culture media (MEM) and inoculated into FRhK-4 cells in 96-well plates. The virus titre was determined by observation of cytopathic effects (CPE) in FRhK-4 cells after 3 days of culture [36, 38].

Q-RT-PCR

Cells were washed twice with PBS, and total RNA was extracted using an RNeasy Mini kit (Qiagen, Germany) in accordance with the manufacturer's instructions. Reverse-transcription was performed using random hexamers with the ThermoScript RT system (Invitrogen, CA). Intracellular viral RNA was quantified using quantitative RT-PCR (Q-RT-PCR) [36, 38, 39], using the forward primer 5'-GCT TAG GCC CTT TGA GAG AGA CA-3' and the reverse primer 5'-GCC AAT GCC AGT AGT GGT GTA AA-3' (final concentration 200 nM), the fluorescent probe 5'-CCT GAT GGC AAA CCT TGC AC-3' and phosphate probe 5'-(LC640)CAC CTG CTC TTA ATT GTT ATT GGC C-3' (final concentration 800 nM). The real-time quantification was carried out using LC Faststart DNA Master Hyb Probes and LightCycler (Roche Diagnostics, USA). PCR conditions employed were 95°C for 10 min and then 50 cycles at 95°C for 10 s, 60°C for 5 s, 72°C for 5 s and 40°C for 30 s. The increase in PCR products was monitored for each amplification cycle by measuring the increase in fluorescence caused by the binding of SYBR Green I to double-stranded DNA. The crossing point values were determined for each sample and specificity of the amplicons was measured by melting curve analysis and visualized by agarose gel electrophoresis. A ten-fold serial dilution of plasmid ranging from 1.5 pg/ml to 1.5 × 10⁶ pg/ml were used as standard and the gene β-actin was used as an endogenous control to normalize for intersample variations in the amount of total RNA.

Determination of Drug Cytotoxic Concentration

Concentration was measured using a standard methylthiazolyldiphenyl-tetrazolium bromide (MTT) assay. The CC₅₀ was determined by fitting data to the logistic equation, as described above; amantadine at 30 μg/ml was used as a toxic control.

Supplemental Data

Supplemental Data for this article is available online at <http://www.chembiol.com/cgi/content/full/12/3/303/DC1/>.

Acknowledgments

This work was supported by the Hong Kong Health, Welfare and Food Bureau under grants from the Research Fund for the Control of Infectious Diseases. R.M.W. was supported by the Area of Excellence Scheme of the University Grants Committee.

Received: August 8, 2004

Revised: December 16, 2004

Accepted: January 12, 2005

Published: March 25, 2005

References

1. Woodward, R.B. (1964). The structure of tetrodotoxin. *Pure Appl. Chem.* 9, 49–74.

2. Wagner, H., Fischer, M., and Lotter, H. (1985). New bufadienolides from *Kalanchoe daigremontiana* Hamet et Perr. (Crassulaceae). *Z. Naturforsch Teil B* 40, 1226–1227.
3. Davies, W.L., Grunert, R.R., Haff, R.F., McGahen, J.W., Neumayer, E.M., Paulshock, M., Watts, J.C., Wood, T.R., Hermann, E.C., and Hoffmann, C.E. (1964). Antiviral activity of 1-Adamantanamine (Amantadine). *Science* 144, 862–863.
4. Schwab, R.S., England, A.C., Jr., Poskanzer, D.C., and Young, R.R. (1969). Amantadine in the treatment of Parkinson's disease. *JAMA* 208, 1168–1170.
5. Wintermeyer, S.M., and Nahata, M.C. (1995). Rimantadine: a clinical perspective. *Ann. Pharmacother.* 29, 299–310.
6. Rosenthal, K.S., Sokol, M.S., Ingram, R.L., Subramanian, R., and Fort, R.C. (1982). Tromantadine: inhibitor of early and late events in herpes simplex virus replication. *Antimicrob. Agents Chemother.* 22, 1031–1036.
7. Kornhuber, J., Weller, M., Schoppmeyer, K., and Riederer, P. (1994). Amantadine and memantine are NMDA receptor antagonists with neuroprotective properties. *J. Neural Transm. Suppl.* 43, 91–104.
8. Kesel, A.J., Sonnenbichler, I., Polborn, K., Gurtler, L., Klinkert, W.E., Modolell, M., Nussler, A.K., and Oberthur, W. (1999). A new antioxidative vitamin B6 analogue modulates pathophysiological cell proliferation and damage. *Bioorg. Med. Chem.* 7, 359–367.
9. Kesel, A.J. (2003). A system of protein target sequences for anti-RNA-viral chemotherapy by a vitamin B6-derived zinc-chelating trioxa-adamantane-triol. *Bioorg. Med. Chem.* 11, 4599–4613.
10. Peiris, J.S., Lai, S.T., Poon, L.L., Guan, Y., Yam, L.Y., Lim, W., Nicholls, J., Yee, W.K., Yan, W.W., Cheung, M.T., et al. (2003). Coronavirus as a possible cause of severe acute respiratory syndrome. *Lancet* 361, 1319–1325.
11. Ksiazek, T.G., Erdman, D., Goldsmith, C.S., Zaki, S.R., Peret, T., Emery, S., Tong, S., Urbani, C., Comer, J.A., Lim, W., et al. (2003). A novel coronavirus associated with severe acute respiratory syndrome. *N. Engl. J. Med.* 348, 1953–1966.
12. Drosten, C., Gunther, S., Preiser, W., van der Werf, S., Brodt, H.R., Becker, S., Rabenau, H., Panning, M., Kolesnikova, L., Fouchier, R.A., et al. (2003). Identification of a novel coronavirus in patients with severe acute respiratory syndrome. *N. Engl. J. Med.* 348, 1967–1976.
13. Rota, P.A., Oberste, M.S., Monroe, S.S., Nix, W.A., Campagnoli, R., Icenogle, J.P., Penaranda, S., Bankamp, B., Maher, K., Chen, M.H., et al. (2003). Characterization of a novel coronavirus associated with severe acute respiratory syndrome. *Science* 300, 1394–1399.
14. Marra, M.A., Jones, S.J., Astell, C.R., Holt, R.A., Brooks-Wilson, A., Butterfield, Y.S., Khattra, J., Asano, J.K., Barber, S.A., Chan, S.Y., et al. (2003). The Genome sequence of the SARS-associated coronavirus. *Science* 300, 1399–1404.
15. Lau, A.C., So, L.K., Mui, F.P., Yung, R.W., Poon, E., Cheung, T.M., and Yam, L.Y. (2004). Outcome of coronavirus-associated severe acute respiratory syndrome using a standard treatment protocol. *Respirology* 9, 173–183.
16. Booth, C.M., Matukas, L.M., Tomlinson, G.A., Rachlis, A.R., Rose, D.B., Dwosh, H.A., Walmsley, S.L., Mazzulli, T., Avendano, M., Derkach, P., et al. (2003). Clinical features and short-term outcomes of 144 patients with SARS in the greater Toronto area. *JAMA* 289, 2801–2809.
17. Cinatl, J., Morgenstern, B., Bauer, G., Chandra, P., Rabenau, H., and Doerr, H.W. (2003). Glycyrrhizin, an active component of liquorice roots, and replication of SARS-associated coronavirus. *Lancet* 361, 2045–2046.
18. Anand, K., Ziebuhr, J., Wadhwani, P., Mesters, J.R., and Hilgenfeld, R. (2003). Coronavirus main proteinase (3CLpro) structure: basis for design of anti-SARS drugs. *Science* 300, 1763–1767.
19. Yang, H., Yang, M., Ding, Y., Liu, Y., Lou, Z., Zhou, Z., Sun, L., Mo, L., Ye, S., Pang, H., et al. (2003). The crystal structures of severe acute respiratory syndrome virus main protease and its complex with an inhibitor. *Proc. Natl. Acad. Sci. USA* 100, 13190–13195.
20. Bacha, U., Barrila, J., Velazquez-Campoy, A., Leavitt, S.A., and Freire, E. (2004). Identification of novel inhibitors of the SARS coronavirus main protease 3CLpro. *Biochemistry* 43, 4906–4912.

21. Wu, C.Y., Jan, J.T., Ma, S.H., Kuo, C.J., Juan, H.F., Cheng, Y.S., Hsu, H.H., Huang, H.C., Wu, D., Brik, A., et al. (2004). Small molecules targeting severe acute respiratory syndrome human coronavirus. *Proc. Natl. Acad. Sci. USA* *101*, 10012–10017.
22. Kao, R.Y., Tsui, W.H., Lee, T.S., Tanner, J.A., Watt, R.M., Huang, J.D., Hu, L., Chen, G., Chen, Z., Zhang, L., et al. (2004). Identification of novel small-molecule inhibitors of severe acute respiratory syndrome-associated coronavirus by chemical genetics. *Chem. Biol.* *11*, 1293–1299.
23. Kleymann, G., Fischer, R., Betz, U.A., Hendrix, M., Bender, W., Schneider, U., Handke, G., Eckenberg, P., Hewlett, G., Pevzner, V., et al. (2002). New helicase-primase inhibitors as drug candidates for the treatment of herpes simplex disease. *Nat. Med.* *8*, 392–398.
24. Crute, J.J., Grygon, C.A., Hargrave, K.D., Simoneau, B., Faucher, A.M., Bolger, G., Kibler, P., Liuzzi, M., and Cordingley, M.G. (2002). Herpes simplex virus helicase-primase inhibitors are active in animal models of human disease. *Nat. Med.* *8*, 386–391.
25. Borowski, P., Schalinski, S., and Schmitz, H. (2002). Nucleotide triphosphatase/helicase of hepatitis C virus as a target for antiviral therapy. *Antiviral Res.* *55*, 397–412.
26. Tanner, J.A., Watt, R.M., Chai, Y.B., Lu, L.Y., Lin, M.C., Peiris, J.S., Poon, L.L., Kung, H.F., and Huang, J.D. (2003). The severe acute respiratory syndrome (SARS) coronavirus NTPase/helicase belongs to a distinct class of 5' to 3' viral helicases. *J. Biol. Chem.* *278*, 39578–39582.
27. Thiel, V., Ivanov, K.A., Putics, A., Hertzog, T., Schelle, B., Bayer, S., Weissbrich, B., Snijder, E.J., Rabenau, H., Doerr, H.W., et al. (2003). Mechanisms and enzymes involved in SARS coronavirus genome expression. *J. Gen. Virol.* *84*, 2305–2315.
28. Ivanov, K.A., Thiel, V., Dobbe, J.C., van der Meer, Y., Snijder, E.J., and Ziebuhr, J. (2004). Multiple enzymatic activities associated with severe acute respiratory syndrome coronavirus helicase. *J. Virol.* *78*, 5619–5632.
29. van Dinten, L.C., van Tol, H., Gorbalenya, A.E., and Snijder, E.J. (2000). The predicted metal-binding region of the arterivirus helicase protein is involved in subgenomic mRNA synthesis, genome replication, and virion biogenesis. *J. Virol.* *74*, 5213–5223.
30. van Marle, G., van Dinten, L.C., Spaan, W.J., Luytjes, W., and Snijder, E.J. (1999). Characterization of an equine arteritis virus replicase mutant defective in subgenomic mRNA synthesis. *J. Virol.* *73*, 5274–5281.
31. Uehara, Y. (2003). Natural product origins of Hsp90 inhibitors. *Curr. Cancer Drug Targets* *3*, 325–330.
32. Wardell, A.D., Errington, W., Ciaramella, G., Merson, J., and McGarvey, M.J. (1999). Characterization and mutational analysis of the helicase and NTPase activities of hepatitis C virus full-length NS3 protein. *J. Gen. Virol.* *80*, 701–709.
33. Baykov, A.A., Evtushenko, O.A., and Avaeva, S.M. (1988). A malachite green procedure for orthophosphate determination and its use in alkaline phosphatase-based enzyme immunoassay. *Anal. Biochem.* *171*, 266–270.
34. Boguszewska-Chachulska, A.M., Krawczyk, M., Stankiewicz, A., Gozdek, A., Haenni, A.L., and Strokovskaya, L. (2004). Direct fluorometric measurement of hepatitis C virus helicase activity. *FEBS Lett.* *567*, 253–258.
35. Biswas, S.B., Chen, P.H., and Biswas, E.E. (1994). Structure and function of *Escherichia coli* DnaB protein: role of the N-terminal domain in helicase activity. *Biochemistry* *33*, 11307–11314.
36. He, M.L., Zheng, B., Peng, Y., Peiris, J.S., Poon, L.L., Yuen, K.Y., Lin, M.C., Kung, H.F., and Guan, Y. (2003). Inhibition of SARS-associated coronavirus infection and replication by RNA interference. *JAMA* *290*, 2665–2666.
37. Porter, D.J. (1998). Inhibition of the hepatitis C virus helicase-associated ATPase activity by the combination of ADP, NaF, MgCl₂, and poly(rU). Two ADP binding sites on the enzyme-nucleic acid complex. *J. Biol. Chem.* *273*, 7390–7396.
38. Zheng, B.J. (2004). Prophylactic and therapeutic effects of small interfering RNA targeting SARS-Coronavirus. *Antivir. Ther.* *9*, 365–374.
39. He, M.L., Wu, J., Chen, Y., Lin, M.C., Lau, G.K., and Kung, H.F. (2002). A new and sensitive method for the quantification of HBV cccDNA by real-time PCR. *Biochem. Biophys. Res. Commun.* *295*, 1102–1107.